

Building formamide and N-substituted formamides from isocyanates on hydrogenated water ices

N. Tieppo¹, P. Redondo^{2,★}, F. Pauzat¹, O. Parisel¹, J.-C. Guillemin^{3,★}, and Y. Ellinger^{3,★}

- ¹ Sorbonne Université, CNRS, Laboratoire de Chimie Théorique, LCT, 75005 Paris, France
- ² Universidad de Valladolid, Facultad de Ciencias (Dpto. QF y QI), 47011-Valladolid, Spain
- ³ Univ Rennes, Ecole Nationale Supérieure de Chimie de Rennes, CNRS, ISCR UMR6226, 35000 Rennes, France

Received 5 May 2024 / Accepted 12 December 2024

ABSTRACT

Context. Many complex organic molecules (COMs) observed in the interstellar medium (ISM) are probably not formed in the gas phase. A large consensus has developed that it could be related to the icy surfaces in this environment.

Aims. We investigate the process of building N-substituted formamides in the ISM by successive additions of atomic hydrogen to isocyanates. The key point is to see whether the pre-adsorption of the atomic hydrogen on the ice surface is a driving vector as it is for the formation of CH₃OH from CO.

Methods. We use quantum numerical simulations, namely density functional theory (DFT) and post Hartree–Fock (p-HF) methods derived from coupled-cluster implementations. Several chemical models are presented: the addition of H directly to the isocyanate in the gas phase, the addition of H to the isocyanate pre-adsorbed on ices, the addition of the isocyanate to the hydrogen pre-adsorbed on ices. These ices are successively simulated by a few water molecules up to full bi-layers of them.

Results. The formation of formamide (NH₂CHO) from the isocyanic acid (HNCO) is taken as a case study. Whatever the level of the calculation and the size of the water cluster supporting the adsorbed isocyanate, the addition of the incoming atomic hydrogen reveals no opportunity to eliminate the energy barrier found in the gas phase. By contrast, the formation of H_2NCHO , as well as CH_3NHCHO or C_2H_5NHCHO , is possible without any barrier on the same ice surfaces, with the express condition that the H atom to be added is already attached to the ice, prior to the attack by the isocyanate species.

Conclusions. There is a way for the N-substituted formamides to be easily built by two successive hydrogenations on ices starting from the isocyanates HNCO, CH₃NCO, and C₂H₅NCO. Some of those species are already detected; if not, they appear as strong candidates worth considering for future observation campaigns. Moreover, this suggests that other hydrogenation processes neglected to date, could be considered when similar pre-conditions are satisfied.

Key words. astrochemistry – molecular processes – ISM: molecules

1. Introduction

Complex organic molecules (COMs) are essentially observed in the gas phase of the interstellar medium (ISM), but this does not imply that they are synthesized solely in this environment. A debate is ongoing about the circumstances of their formation and especially about the possible role of a solid partner such as interstellar icy grains.

Among the molecules of interest for astrobiology, the origin of which is still uncertain, are formamide and the N-substituted formamides. Formamide NH₂CHO and N-methyl-formamide CH₃NHCHO have been detected, respectively, by Rubin et al. (1971) and Belloche et al. (2017). Their potential precursors, the isocyanates HNCO and CH₃NCO, have been observed by Snyder & Buhl (1972), Halfen et al. (2015), and Cernicharo et al. (2016). The following term of the series, C₂H₅NCO, was also detected by Rodríguez-Almeida et al. (2021). It should be emphasized that these three isocyanates satisfy the minimum energy principle (MEP). This principle, according to which the most abundant compound in a given series of isomers should be the most thermodynamically stable, is a pragmatic rule verified in up to 90% of the molecules in the ISM (Lattelais et al. 2009). Applied to the isomers of the CHON generic formula, isocyanic

acid (HNCO), cyanic acid (HOCN), fulminic acid (HCNO) and isofulminic acid (HONC), all of which are closed-shell molecules, this results in the following stability ordering:

HNCO > HOCN > HCNO > HONC (Lattelais et al. 2015;

Fourté et al. 2020). This order on the energy scale is in per

Fourré et al. 2020). This order on the energy scale is in perfect accordance with the relative abundances observed of HNCO (Snyder & Buhl 1972) HOCN (Brünken et al. 2009), with a 0.03 to 0.003 abundance ratio, less abundant HCNO (Marcelino et al. 2008), and the non-observation of HONC, although it was characterized in the laboratory (Mladenovic et al. 2009).

The most stable isomer, HNCO, which could be seen as a precursor of an amide linkage, has been detected in numerous sources: first in Sgr B2, about fifty years ago (Snyder & Buhl 1972), then in cold dense cores (Brown 1981; Marcelino et al. 2008; López-Sepulcre et al. 2015), in hot cores (Snyder & Buhl 1972; Churchwell et al. 1986; Martín et al. 2008) and hot corinos (López-Sepulcre et al. 2015), in photon-dominated regions (Jansen et al. 1995) in diffuse clouds (Turner et al. 1999), in the direction of the galactic center (Cummins et al. 1986; Kuan & Snyder 1996), in molecular shocks (Mendoza et al. 2014), and in external galaxies (Meier & Turner 2005; Martín et al. 2008).

A correlation has also been found between the abundances of H_2NCHO and HNCO in the gas phase. The hydrogenation of isocyanic acid was proposed by López-Sepulcre et al. (2015), as a likely formation route to formamide. Belloche et al. also

^{*} Corresponding authors; pilar.redondo@uva.es; jean-claude.guillemin@ensc-rennes.fr; yves.ellinger@ensc-rennes.fr

suggested that production of N-methyl-formamide may plausibly occur on grains through the hydrogenation of CH₃NCO (Belloche et al. 2017). Then, the question of building N-substituted formamides from the isocyanates by successive additions of atomic hydrogens is altogether logical and challenging. The crucial point is whether or not an energy barrier sits along the hydrogenation path.

In a recent publication (Tieppo et al. 2023), we showed that the successive hydrogenations of CO into methanol by atomic H, resulting in

is free of an activation barrier at every step of the process under the condition that the added hydrogen atom, H, is already attached at the surface of the ice. Such a finding would provide an alternative to the current view (Tielens & Hagen 1982) that activation barriers do exist for the first and third steps of the hydrogenation mechanism. An exhaustive review of the subject can also be found in Tielens & Whittet (1997).

More recently, a quantum study of the radiative association of H and CO to form the HCO molecule was performed within a time-independent approach (Stoecklin et al. 2018). The results of this study demonstrate that the gas-phase H+CO radiative association cannot be the process at the origin of the sequence leading to the formation of methanol in a cold interstellar medium (ISM).

The role of the pre-adsorption of H leading to the disappearance of the activation barriers in the hydrogenation of the CO double bond is thus worthy of an in-depth investigation in view of a possible extension to other types of insaturations. This is presented below on the cumulene fragment (NCO), which is a possible precursor of amides.

After a brief presentation of the computational protocol, we focus on the formation of formamide and a series of N-substituted formamides, all of whose isocyanate precursors satisfy the MEP: formamide (HNHCHO), N-methylformamide (CH₃NHCHO), and N-ethylformamide (C₂H₅NHCHO).

2. Methods and chemical models

For DFT calculations, we used, alternatively, the MPWB1K (Adamo & Barone 1998) and the M06-2X (Zhao & Truhlar 2008) exchange-correlation functionals with the aug-cc-pVTZ, aug-cc-pVQZ, or 6-311++(3df,2p) basis sets. The reactants of each stage are brought together and optimized to follow the reaction path.

For the smaller structures, post-Hartree–Fock (p-HF) calculations are also done at the coupled cluster single and double excitations (CCSD) (Bartlett & Shavitt 1977) or coupled cluster single, double and triple excitations (CCSD(T)) (Raghavachari et al. 1989) levels with the aug-cc-pVTZ or aug-cc-pVQZ basis set, following the same protocol. The use of diffuse atomic functions is justified since they are able to better describe long-range and weak interactions. Throughout this work, the calculations are performed using the methods and basis sets coupled with geometry optimization gradient procedures, as implemented in the Gaussian16 software (Frisch et al. 2016).

In order to consider the possible influence of the environment, we checked for a possible role of water ice. First, a few molecules of H₂O are introduced as a support in the reaction

process, then full H₂O bi-layers are considered. In that case, all atoms are frozen, except those of the immediate neighboring water molecules of the reaction site.

All reported stationary points on the reaction paths (equilibrium structures and transition states) are true minima, as verified by vibrational analysis. The absence of activation barriers is asserted following three different protocols, namely, relaxed scan, intrinsic reaction coordinate survey, and direct optimization search starting from the transition states already known, if any, from the H-only atomic hydrogenation.

3. Gas-phase reactions from HNCO to H₂NCHO

In this work, the process taken as a case study is the formation of the simplest amide, NH₂CHO by two successive hydrogenations of the HNCO isocyanate. It is done according to the following series of reactions:

$$HNCO + H \rightarrow H_2NCO$$
 (1)

$$H_2NCO + H \rightarrow H_2NCHO$$
 (2)

or

$$HNCO + H \rightarrow HNCHO$$
 (3)

$$HNCHO + H \rightarrow H_2NCHO.$$
 (4)

Both ways, that is to say (1+2) and (3+4), proceed through different species to reach the same end product: H_2NCHO . Two situations are considered thereafter: gas-phase reactions and catalytic reactions with the active participation of icy grains' mantles.

We start with the hydrogenation processes taking both HNCO and H reactants as free flyers. For this, we employ different ab initio and DFT methodologies. We located the different intermediates and transition states of the (HNCO + H + H) system along the reaction paths that could lead to formamide. The results at the different levels of calculations are collected in Table 1, with the energy profile shown in Fig. 1.

The addition of the first hydrogen atom goes through either TS1 or TS3, depending on whether H connects to the nitrogen or to the carbon atom 1 . The first situation leads to a significantly lower transition state TS1 and a more stable intermediate free-radical H_2NCO than the HNCHO isomer.

The addition of the second H (reactions 2 and 4) are radicalradical processes in both cases. This type of reaction is wellknown to be barrier-less and is not discussed any further here.

It should be stressed that the results detailed in Table 1 remain steady whatever the level of theory chosen for the calculations. Both energy barriers remain practically constant with the methodologies within a margin of at most 10%. Thus, the averaged energy barriers obtained for steps (1) and (3) are 9.0 and $15.7 \pm 1.0 \, \text{kcal/mol}$, respectively, for TS1 and TS3.

Taking into account the temperature conditions of the cold ISM, the energy levels needed to reach the transition states of the first step of the processes are too high to be ignored in both cases. This means that in the gas phase of the cold ISM, none of these reactions will occur since efficient tunneling appears highly improbable.

4. Addition of H to HNCO adsorbed on ice

In order to evaluate the possible role of solid particles, we considered model surfaces of icy grain mantles. We first introduce

¹ These generic names, TS1 and TS3, refer to the reaction number in the above chemical network and are used throughout the paper.

Table 1. Stationary points along gas-phase reaction path from HNCO to NH₂CHO.

Method ^(***)	CCSD(T)(*)/B1	CCSD(T)(*)/B2	CCSD(T)(**)/B1	CCSD(T)(**)/B2	MPWB1K/B1	M06-2X/B1
$HNCO(^{1}A') + 2H(^{2}S)$	0.0	0.0	0.0	0.0	0.0	0.0
$TS1 (^2A') + H (^2S)$	9.4	9.4	8.0	7.9	9.3	9.9
$NH_2CO(^2A') + H(^2S)$	-25.9	-26.0	-26.7	-26.9	-27.1	-25.1
$TS3 (^2A') + H (^2S)$	16.5	16.6	14.8	14.9	15.7	15.8
$HNCHO(^{2}A) + H(^{2}S)$	-6.9	-6.2	-6.4	-5.8	-6.3	-5.9
$NH_2CHO(^1A')$	-117.7	-118.3	-118.4	-119.1	-117.9	-116.9

Notes. (*)Calculated from the geometries optimized at the CCSD/aug-cc-pVTZ level. (**)Calculated from the geometries optimized at the MP2/aug-cc-pVTZ level. Basis: B1 = aug-cc-pVTZ; B2 = aug-cc-pVQZ. (***)Energy differences along the reaction paths include zero-point vibrational energies in kcal/mol.

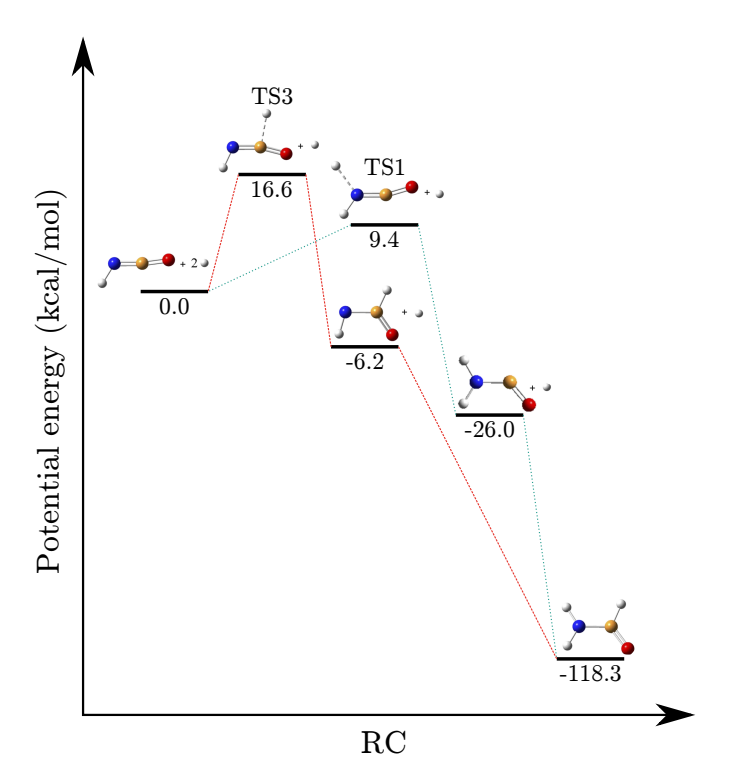


Fig. 1. Gas-phase reaction profile for successive hydrogenations of HNCO to obtain H₂NCHO. Calculations performed at the CCSD(T)/aug-cc-pVQZ level. Relative energies including zero-point vibrational energies in kcal/mol.

an increasing number n of H_2O molecules, (n = 1, 2, 3), and then 24 or 48 H_2O clusters as the reaction support. Each of the small clusters is optimized as an independent monomer, dimer, or trimer.

The larger ones are directly cut into (Ih) crystalline ice. In all cases, HNCO is attached to the cluster before the reactions begin. When the addition of H to form NH_2CO or HNCHO proceeds through transition states, those, as in the previous section, are referred to as TS1 and TS3, respectively.

4.1. HNCO adsorbed on small H₂O clusters

Full results of the hydrogention of HNCO adsorbed on $(H_2O)n$ (n=1,2,3) clusters are reported in Table 2 for all types of structures located along the reaction coordinate. Figure 2 exhibits the case n=2 as a significant example, showing that no noticeable change from the gas phase occurred:

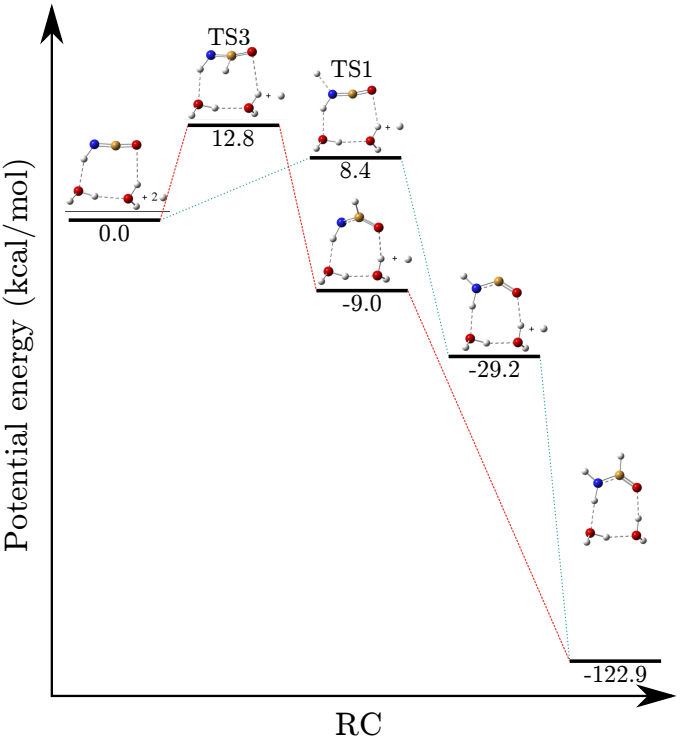


Fig. 2. Reaction profile for successive hydrogenations of HNCO to obtain NH_2CHO , starting from HNCO attached to two water molecules. This was calculated at the CCSD(T)/aug-cc-pVTZ level. Relative energies including zero-point vibrational energies are in kcal/mol.

- (i) Two clear energy barriers (larger than 8 and 12 kcal/mol, corresponding to TS1 and TS3 respectively) are present on the way to the first hydrogenation of HNCO.
- (ii) Once the intermediate radicals H₂NCO and HNCHO have been obtained, the addition of the second hydrogen atom to give NH₂CHO follows without any transition state to oppose its formation.

The cross-checks of the different computational levels show an unchanged picture of the overall processes. The relative energies calculated at the DFT and p-HF levels are found close to each other for the reactions supported by one, two, and three H_2O molecules. In view of the constancy of the barriers, we can assert that changes between the cases $n=1,\,2,\,3$ are minor. In conclusion, the point is, once more, that it is not possible to ignore the barriers and to pass over in the cold ISM.

Table 2. Critical points of the hydrogenation path on ice models from HNCO to NH₂CHO.

Method (**)	n	CCSD(T)(*)/B1	CCSD(T)(*)/B2	M062X/B3	MPWB1K/B3
$HNCO(^{1}A') + 2H(^{2}S)$	1	0.0	0.0	0.0	0.0
	2	0.0		0.0	0.0
	3	0.0		0.0	0.0
$HNCO-Layer (^1A) + 2 H (^2S)$	48			0.0	0.0
$TS1 (^2A') + H(^2S)$	1	9.1	9.0	10.0	9.5
	2	8.4		9.2	8.8
	3	8.0		8.8	8.5
$TS1-Layer (^2A) + H(^2S)$	48			8.7	8.5
$\overline{NH_2CO(^2A') + H(^2S)}$	1	-28.9	-29.0	-28.6	-30.3
	2	-29.2		-28.6	-30.5
	3	-27.7		-26.9	-29.2
NH_2CO -Layer ($^2A'$) + H (2S)	48			-28.0	-28.4
$TS3 (^2A) + H(^2S)$	1	17.8	17.7	14.7	14.7
	2	12.8		10.8	11.6
	3	12.3		9.8	11.4
TS3-Layer (2 A) + H (2 S)	48			7.9	11.4
$\frac{1}{1} + \frac{1}{1} + \frac{1}$	1	-8.1	-7.5	-6.9	-8.7
, , , ,	2	-9.0		-7.6	-9.2
	3	-8.4		-6.8	-8.6
$HNCHO-Layer(^2A) + H(^2S)$	48			-6.8	-8.3
NH ₂ CHO(¹ A')	1	-122.1	-122.7	-121.9	-122.6
	2	-122.9		-122.3	-123.3
	3	-121.2		-120.4	-121.7
NH ₂ CHO-Layer (¹ A)	48			-121.1	-121.1

Notes. (*) Geometries optimized at the MP2/aug-cc-pVTZ level. Basis sets: B1 = aug-cc-pVTZ; B2 = aug-cc-pVQZ; B3 = 6-311++G(3df,2p); $n = number of supporting <math>H_2O$. (**) Energy differences along the reaction paths include zero-point vibrational energies in kcal/mol.

4.2. HNCO adsorbed on H₂O crystalline ice models

In order to have what we thought a more realistic description of the surface on which the hydrogenation reactions take place, we built a structure of 24 or 48 water molecules. This, in accordance with our previous works on the reactivity at the top of ice (Redondo et al. 2020, 2021).

The first water-ice model surface is obtained by an appropriate cut of 24 $\rm H_2O$ molecules assembled in the form of six fused cyclohexane-like structures to mimic a significant part of the surface of the (Ih) crystalline ice. An extension of the model can be obtained by superimposing two of these structures (48 $\rm H_2O$ molecules) to tentatively apprehend the possible role of the underlying bulk. Figure 3 shows the $\rm H_2NCO$ most stable intermediate adsorbed on the top surface of the (Ih) water ice.

In our previous works, this ice modeling has proven to give similar results to those obtained by a periodic solid-state DFT with specific formalisms accounting for weak interactions in systems of infinite dimensions (Redondo et al. 2020, 2021). It can also be seen in Table 2 that the relative energies calculated for H_2NCO and HNCHO at the DFT and p-HF levels are found close to each other for the reactions supported by one, two, and three H_2O molecules. Thus, given those results and the dimensions of the extended crystalline models, we limited the computational size of the relative energies at the M062X and MPWB1K levels.

The results of the calculated stationary points are collected in Table 2; this is done in Table 3 for the largest representation

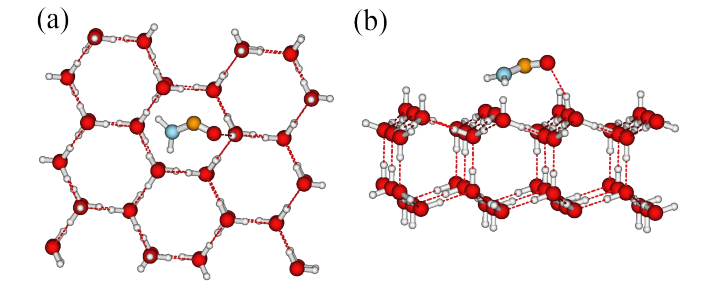


Fig. 3. Most stable H₂NCO intermediate radical adsorbed on the top surface of (Ih) water ice. (a) Top view. (b) Side view.

of the ices. They show no significant change on the hydrogenation profile of reactions (1) and (3). The two transition states still exist for the first hydrogenation steps with significant energy barriers whatever the method and the chemical model. The values reported in Table 3 show that the use of models involving either 24 or 48 H₂O water molecules has no real influence; neither does the choice to optimize – more or less – the environment by including two or six surrounding water molecules in the optimization scheme. The choice of the methodology has only a marginal effect. At this point, the conclusion is that this hydrogenation process does not look probable in the cold ISM conditions: neither in the gas phase, nor when the isocyanate is adsorbed on an icy surface.

Table 3. Influence of optimization on the reaction path from HNCO first adsorbed on ice lave	avers to NH ₂ CHO.
---	-------------------------------

	24 H ₂ O cluster				48 H ₂ O cluster			
Method	M062X ^(*) /B1		MPWB1K(**)/B1		M062X ^(*) /B3		MPWB1K ^(**) /B3	
n opt	2	6	2	6	2	6	2	6
$\frac{1}{1}$ HNCO-Layer(1 A) + 2 H(2 S)	0.0	0.0	0.0	0.0	0.0	0.0	0.0	0.0
$TS1 (^2A) + H(^2S)$	8.1	8.2	7.9	7.8	8.7	8.7	8.5	8.2
$NH_2CO-Layer(^2A) + H(^2S)$	-25.7	-27.6	-27.7	-29.1	-28.0	-27.4	-28.4	-28.2
$TS3 (^2A) + H(^2S)$	11.2	10.4	14.8	14.4	7.9	7.9	11.4	11.4
$HNCHO-Layer(^2A) + H(^2S)$	-3.3	-4.0	-4.8	-5.4	-6.8	-6.5	-8.3	-8.3
NH ₂ CHO-Layer(¹ A)	-120.6	-120.5	-121.0	-120.5	-121.1	-120.9	-121.1	-121.5

Notes. (*) Geometries optimized at the M062X/6-31++G(d,p) level. (**) Geometries optimized at the MPWB1K/6-31++G(d,p) level. Basis sets: B1 = aug-cc-pVTZ B3 = 6-311++G(3df,2p); n opt = number of H₂O of the surface considered in the geometry optimization. Relative energies including zero-point vibrational energies are in kcal/mol.

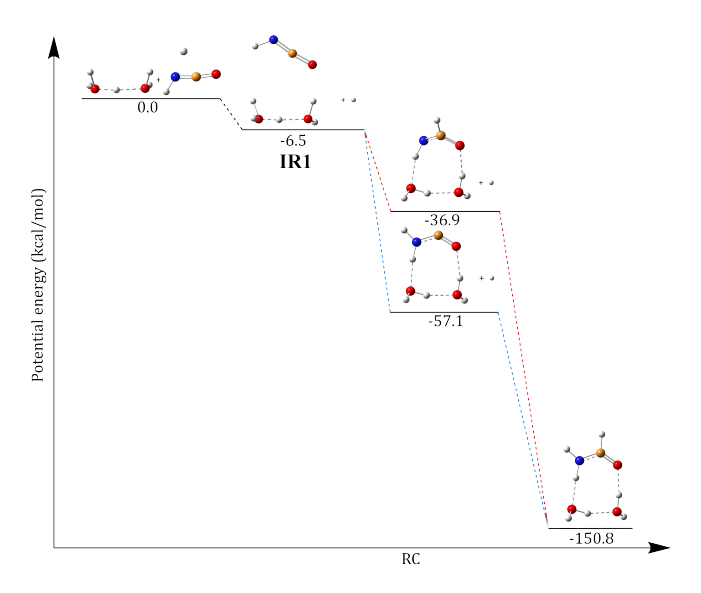


Fig. 4. Reaction profile for successive hydrogenations of HNCO to obtain NH $_2$ CHO, starting from a hydrogen atom attached to two water molecules calculated at the CCSD(T)/aug-cc-pVTZ level. Relative energies including zero-point vibrational energies are in kcal/mol.

5. Addition of HNCO to H already attached to ice

It was recently shown (Tieppo et al. 2023) that bi-molecular reactions at a solid ice surface could strongly depend on which of the reactants is first attached to the support. This attachment ordering was found to be strongly selective for the addition reaction. Hereafter, we consider the reaction starting with the hydrogen atom linked to the solid ice; we sought some similarity with the hydrogenation of CO into methanol. This required looking at the hydrogenation process from a different angle.

The relative energies of the localized stationary points for the hydrogenation process of HNCO in the presence of the hydrogen first attached to one, two, three, and 48 H₂O molecules (ice bilayer surface) are given in the Appendix (Table A.1).

The first step is the formation of a metastable IR1 intermediate complex between the incoming HNCO molecule and the water molecules supporting the hydrogen attached to the surface. The hydrogenation of HNCO at the nitrogen or carbon atom by the adsorbed hydrogen to give NH₂CO or HNCHO takes place directly (i.e., without an activation barrier), as illustrated in Fig. 4 with the case of a small cluster of two water molecules.

This is true whatever the representation of ice (small cluster or layer). Then, once NH₂CO or HNCHO radicals have been reached, the second hydrogenation step to give formamide proceeds without an activation barrier². The general trend is similar in all cases: no barrier of any kind appears on the reaction path.

As in the preceding calculations (gas phase and HNCO attached to ices), the numbers obtained for the successive models are rather steady. Relying on the results obtained for the reaction with HNCO attached to the ices (Table 3) and for the sake of consistency, we used the same model of 48 H₂O molecules with two neighboring molecules optimized in the simulation of the surface ice layer. We indeed observed that the optimization of (Layer + HNCO) was almost independent of the model (to unburden the presentation, computational details are given in Table A.1).

However, it might not be identical for the (Layer + H) stabilization. Indeed, when one bi-layer is used and six water molecules are optimized, the hydrogen atom becomes part of the layer structure, which could lead to an extra stabilization of the starting point ([Layer-H] + HNCO + H). The effect should be reduced when using a double bi-layer surface model. When two bi-layers are taken into consideration (48 $\rm H_2O$ molecules), the lower bi-layer, which plays the role of the bulk inside the ice, prevents the surface from changing significantly when the H atom is adsorbed; this ensures a closer description to a real surface. Using a bi-layer that is harder to distort and only allowing two neighboring molecules to adapt helps avoid the artifact.

Finally, we can conclude that this process should be feasible in the ISM provided the atomic hydrogen is attached beforehand at the surface of solid water ice. Consequently, we will investigate the same mechanism with regard to the R-NCO family of molecules.

6. Hydrogenation of R-NCO isocyanates on ice

The isocyanate molecule HNCO is known to be the most thermodynamically stable species possible with the tetra-atomic CHON raw formula (Lattelais et al. 2015). In a similar way, the recently observed CH₃NCO (Fourré et al. 2020) and C₂H₅NCO are the most stable isomers of their respective raw formulas (Lattelais et al. 2009; Halfen et al. 2015; Cernicharo et al. 2016; Rodríguez-Almeida et al. 2021).

 $^{^2}$ It means that the second addition of H can be obtained with either a hydrogen coming from the gas-phase or an H already attached to the ice.

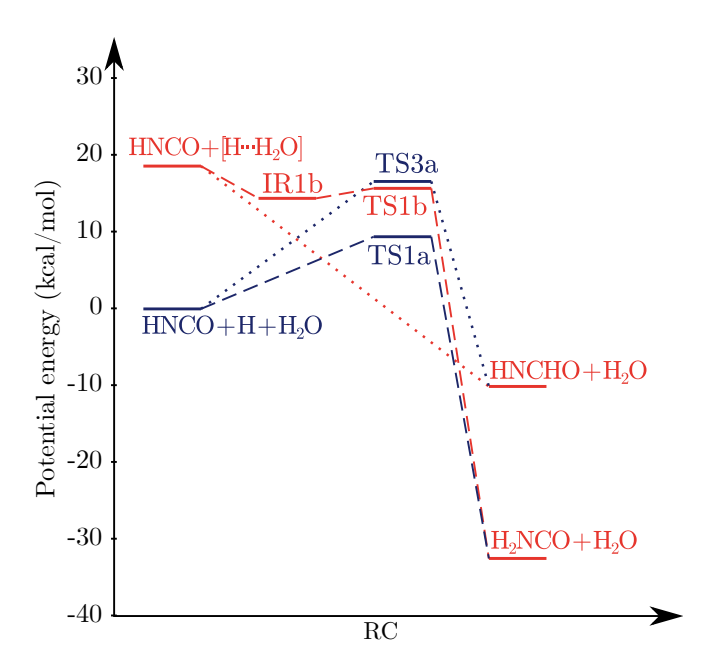


Fig. 5. Comparison of HNCO hydrogenation by an H adsorbed on ice (b path in red) modeled by $[H...OH_2]$; HNCO hydrogenation modeled by a free H atom (a path in blue) at M06-2X/aug-cc-pVTZ level.

Since the hydrogenation of HNCO leading to formamide without any energetic supply is possible on an icy surface with a hydrogen atom pre-attached, we considered generalizing the same mechanism with regard to the R-NCO family of molecules. However, the preceding calculations are rather heavy and time-consuming to carry out for more complex systems. A simpler model would thus be welcome. To this end, we take [H . . . OH₂] as a local representation of the hydrogenation reactive site able to account for the catalytic role played by water ice when an atom H is attached at the surface. This synthetic model has proven to be a valuable tool to rationalize the formation of CH₃OH by successive atomic hydrogenations of CO (Tieppo et al. 2023).

Therefore, we applied this simple approach to the hydrogenation of HNCO. The results are shown in Fig. 5 and Table 4. Within this model, both NH₂CO and NHCHO intermediate radicals can be reached. Taking a closer look at the NH₂CO reaction path (see Fig. 5) reveals that the reaction begins with the formation of a complex (IR1b) between [H . . . H₂O] and HNCO followed by a "submerged" transition state (TS1b). Such a transition state is also more stable than the reactants, so the energy released by forming the intermediate species is large enough to pass over the activation barrier. The second hydrogenation is barrier-less whatever the model, as it was already for the gas phase process. The results obtained with this approach agree with that shown in the previous section for the hydrogen absorbed on one, two, three, or 48 (a two-bi-layer surface) H₂O molecules. Consequently, we planned to use our synthetic [H . . . OH₂] model for the study of hydrogenations in the case of more complex isocyanates into N-alkyl formamides.

Before looking at hydrogenation mechanisms in detail, we regard the atomic charge distribution of each starting isocyanate obtained through the Mulliken population analysis:

$$\begin{split} &H{-}N^{-0.20}{=}C^{+0.27}{=}O^{-0.27}\\ &CH_3{-}N^{+0.20}{=}C^{-0.13}{=}O^{-0.41}\\ &CH_3CH_2{-}N^{+0.20}{=}C^{-0.22}{=}O^{-0.51}. \end{split}$$

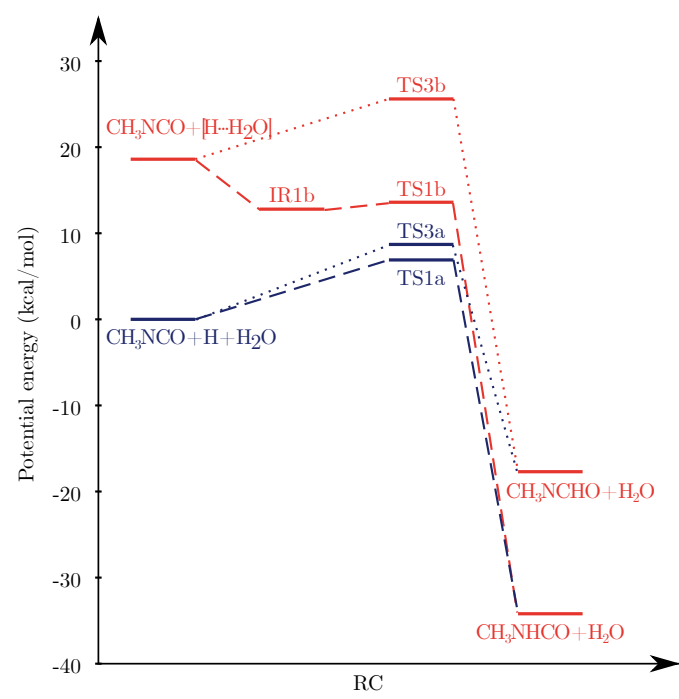


Fig. 6. Comparison of CH_3NCO hydrogenation by an H adsorbed on ice (b path in red), modeled by $[H \dots OH_2]$, and CH_3NCO hydrogenation by a free H atom (a path in blue; calculated at the M06-2X/aug-cc-pVTZ level).

There is a net difference between HNCO and the substituted $\mathrm{CH_3NCO}$ and $\mathrm{C_2H_5NCO}$ isocyanates. The electronic charge on N is negative if it is bound to a single H, whereas it is positive when it is bound to an alkyl fragment. We have to keep in mind that this charge reversal might have an impact on the product favored by a charge-controlled type of reaction.

6.1. From CH₃NCO to CH₃NHCHO

The double hydrogenation of the first N-alkyl isocyanate (CH₃NCO) leads to the formation of N-methyl formamide, which is the second most stable C₂H₅NO isomer after acetamide (Fourré et al. 2020). Following observations on Sgr B2 (Belloche et al. 2017, 2019), CH₃NHCHO is more abundant than expected if one compares with the abundance of the corresponding derivative of HNCO. The question now is whether or not the preadsorption of atomic H is still influential when the hydrogen of the isocyanate is substituted by CH₃.

The situation is clarified in Fig. 6, where the process in which H is not pre-adsorbed is shown for comparison. We present the reaction path from CH₃NCO to CH₃NHCHO by successive hydrogenation at the surface of water-ice grain mantles. For such a purpose, we trusted the efficient synthetic model developed previously to represent an atomic hydrogen pre-attached at the surface of water ice by [H...OH₂].

The first stage could lead to two products: CH₃HNCO and CH₃NCHO equivalent to reactions (1) and (3), respectively. However, the presence of CH₃ instead of a single H leads to a clear selectivity as the transfer of the adsorbed hydrogen on the carbon has an activation barrier of about 7 kcal/mol (see Table 4), whereas the transfer on the nitrogen is barrier-less. The second stages (2) and (4) are barrier-less, both in the gas phase and in our model.

Table 4. Reaction enthalpy (ΔH) in kcal/mol along the reaction paths for R-NCO by [H . . . OH₂] leading to RNH-formamides.

R =	I	H	C	C_2H_5	
Method (*)	CCSD	M06-2X	CCSD	M06-2X	M06-2X
Basis set	aug-cc-pVTZ	aug-cc-pVTZ	aug-cc-pVTZ	aug-cc-pVTZ	aug-cc-pVTZ
	-53.66	-51.07	-55.64	-52.81	-52.13
	-34.91	-28.68	-41.34	-36.28	-36.14
	-118.49	-118.36	-118.63	-118.51	-117.83
	-137.24	-140.75	-132.93	-135.04	-133.82
$[H_2O \dots H] + R-NCO \longrightarrow IR1b$ $[H_2O \dots H] + R-NCO \longrightarrow TS1b$ $[H_2O \dots H] + R-NCO \longrightarrow TS3b$	-3.16 -0.57	-4.14 -2.87	-4.12 -1.36	-5.86 -5.01 7.00	-7.13 -6.22 6.99

Notes. (*) Considering the ISM's low temperature, the role of zero-point vibrational energies has been neglected, allowing us to save on computing time.

6.2. From C_2H_5NCO to C_2H_5NHCHO

The third isocyanate in the series is C₂H₅NCO. Though identified in the ISM, none of its hydrogenated daughters have been observed. So, it is particularly interesting to check whether its hydrogenation process is similar to those already found in the same family. CH₃NCO and C₂H₅NCO, presenting similar highenergy orbitals and electronic distribution, should also present a close reactivity. This is illustrated in Figure 7, where reaction paths with H as a free-flyer (path in blue) and H attached to the model surface (path in red) are compared.

Using the same methodology, we find the following:

- For H as a free-flyer, we have activation barriers for hydrogenation on both N and C atoms passing by transition states TS_{1a} or TS_{3a} respectively.
- For H attached to the ice surface, we obtain the first hydrogenation of C_2H_5NCO on the N atom without any energy barrier, while the hydrogenation on C shows a 7 kcal/mol barrier (see Table A.1).

Since the second hydrogenation steps (radical-radical process) are barrier-less as usual, whatever the environment conditions, there is always a possibility of formation of Nethylformamide through the following path:

$$\begin{split} &C_2H_5NCO + [H...OH_2] \rightarrow C_2H_5NHCO + H_2O \\ &C_2H_5NHCO + [H...OH_2] \rightarrow C_2H_5NHCHO + H_2O. \end{split}$$

Then, a search for C₂H₅NHCHO in the environment where ethylisocyanate has been detected is fully pertinent.

7. Astrophysical implications and conclusion

Two simple amides, formamide and N-methylformamide, have been detected in the ISM, and it has been proposed that they may be formed by the hydrogenation of the corresponding isocyanate. Isocyanic acid and methyl- and ethyl-isocyanate have also been detected and may therefore be precursors of the two detected formamides and N-methylformamide, respectively. However, laboratory attempts to reduce HNCO to formamide have failed so far (Noble et al. 2015). HNCO ice was bombarded by H atoms with a flux of about 10¹⁴ cm⁻² s⁻¹ at about 300 K produced in a molecular hydrogen plasma generated by a 2.45 GHz microwave discharge. Here, we clearly demonstrate that such a reaction must cross an activation barrier to occur under various experimental

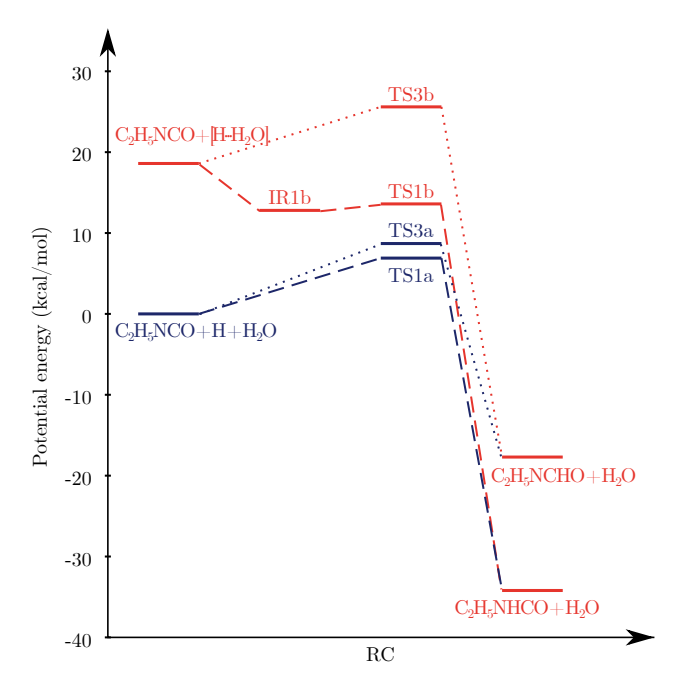


Fig. 7. Comparison of C_2H_5NCO hydrogenation by an H adsorbed on ice (b path in red) modeled by $[H \dots OH_2]$ and C_2H_5NCO hydrogenation by a free H atom (a path in blue; results at M06-2X/aug-cc-pVTZ level).

conditions. We propose that the pre-adsorption of atomic hydrogen on the ice surface can effectively reduce hydrocyanic acid into formamide and methyl- and ethyl-isocyanate into methyland ethyl-formamide, respectively. In another theoretical study, we already showed how carbon monoxide can be reduced in methanol in several steps without an activation barrier (Tieppo et al. 2023) in contrast to the reported experimental approaches (Hirakoa et al. 1994; Watanabe & Kouchi 2002; Fuchs et al. 2009; Pirim & Krim 2011). Such an approach paves the way for the reconsideration of several other experimentally unsuccessful hydrogenation reactions to date, such as the reduction of aldehydes and ketones in the corresponding alcohols (Jonusas et al. 2017) or of nitriles in imines and then amines (Nguyen et al. 2019; Krim et al. 2019), while only the reductions of formaldehyde and hydrogen cyanide (Theule et al. 2011) have been experimentally successful. On the other hand, a compound such as glyoxal, which only led to the formation of carbon monoxide and formaldehyde and then methanol (Leroux et al. 2020), could be a precursor of glycolaldehyde and then ethylene glycol. This radically changes the possible reactions at low temperatures in the ISM and gives new precursors for N-substituted formamides, alcohols (ethanol, propanol, isopropanol), imines (ethanimine, N-cyanomethanimine and iminoacetonitrile), and amines (ethylamine, vinylamine) already detected in the ISM and for which a corresponding unsaturated precursor has been detected. In parallel with these studies, laboratory hydrogenations under these particular conditions are necessary to provide an experimental demonstration of this theoretical work.

Moreover, it is worth reminding that the aim of this work was to explore the formation of alkyl N-substituted formamides R-NHCHO by double successive hydrogenations of isocyanates R-NCO using different computational models. Taking HNCO as case study, we found the first important result: the addition of atomic hydrogen directly on the isocyanate in the gas phase shows an activation barrier high enough to oppose the reaction significantly. When HNCO is attached to the ice (small cluster or full layers of water molecules), the same type of energy barrier exists on the chemical path to the formation of the associated formamide NH₂CHO. This barrier is also too high to be surmounted in the cold ISM.

Due to the fact that the abundance of hydrogen is orders of magnitude greater than that of the isocyanates, we thought that another type of reaction was worth investigating: namely, the addition of HNCO onto a hydrogen already attached to the ice. In such circumstances, it appears that the whole process is free of activation energies. Moreover, when [H ...OH₂] is considered as a local representation of the hydrogenation reactive site, capable of describing the catalytic function of water ice when hydrogen is bonded to the surface, similar results are obtained for HNCO hydrogenation.

In view of this questioning result, we checked the possible generalization of the above catalytic process for larger entities of the same chemical family, substituting the H of HNCO by CH_3 and C_2H_5 . If the attacks by an H free-flyer also reveal energetic barriers making the process most unlikely in the cold ISM, the reactions of the isocyanates with a H already attached on ices, modeled by a single water molecule, also proceed without any constraint. In particular, it allows the barrier-less formation of CH_3NHCHO already observed in the ISM.

In conclusion, the decisive point is that the presence of H atoms pre-attached to the ice surface can generate the formation of metastable complexes with different molecules. Those complexes behave as starting points on the global energy scale and thus make the hydrogenation mechanism barrier-less.

Acknowledgements. This work was supported by CNES and CNRS national program PCMI. PR acknowledges support from the Spanish Ministerio de Ciencia e Innovacion (PID2020-117742GB-I00). We thank O. Tasseau (Ensc-Rennes) for computational assistance.

References

Adamo, C., & Barone, V. 1998, J. Chem. Physics, 108, 664

Bartlett, R. J., & Shavitt, I. 1977, Chem. Phys. Lett., 50, 190

Belloche, A., Meshcheryakov, A. A., Garrod, R. T., et al. 2017, A&A, 601,

```
Belloche, A., Garrod, R. T., Müller, H. S. P., et al. 2019, A&A, 628, A1
Brown, R. L., 1981, ApJ, 248, L119
Brünken, S., Gottlieb, C. A., McCarthy, M. C., & Thaddeus, P. 2009, ApJ, 697,
Cernicharo, J., Kisiel, Z., Tercero, B., et al. 2016, A&A, 587, L4
Churchwell, E., Wood, D., Myers, P. C., & Myers, R. V. 1986, ApJ, 305,
Cummins, S. E., Thaddeus, P., & Linke, R. A. 1986, ApJS, 60, 819
Fourré, I., Matz, O., Ellinger, Y., & Guillemin, J.-C. 2020, A&A, 639, A16
Frisch, M. J., Trucks, G. W., Schlegel, H. B., et al. 2016, Gaussian16 Revision
  C.01
Fuchs, G. W., Cuppen, H. M., Ioppolo, S., et al. 2009, A&A, 505, 629
Halfen, D. T., Ilyushin, V. V., & Ziurys, L. M. 2015, ApJ, 812, L5
Hiraoka, K., Ohashi, N., Kihara, Y., et al. 1994, Chem. Phys. Lett., 229, 408
Jansen, D. J., Spaans, M., Hogerheijde, M. R., & van Dishoeck, E. F. 1995, A&A,
  303, 541
Jonusas, M., Guillemin, J.-C., & Krim, L. 2017, MNRAS, 468, 4592
Krim, L., Guillemin, J.-C., & Woon, D. E. 2019, MNRAS, 485, 5210
Kuan, Y.-J., & Snyder, L. E. 1996, ApJ, 470, 981
Lattelais, M., Pauzat, F., Ellinger, Y., & Ceccarelli, C. 2009, ApJ, 696, L133
Lattelais, M., Pauzat, F., Ellinger, Y., & Ceccarelli, C. 2015, A&A, 578,
Leroux, K., Guillemin, J.-C., & Krim, L. 2020, MNRAS, 491, 289
López-Sepulcre, A., Jaber, A. A., Mendoza, E., et al. 2015, MNRAS, 449,
Marcelino, N., Cernicharo, J., Tercero, B., & Roueff, E. 2008, ApJ, 690, L27
Marcelino, N., Brünken, S., Cernicharo, J., et al. 2010, A&A, 516, A105
Martín, S., Requena-Torres, M. A., Martín-Pintado, J., & Mauersberger, R. 2008,
   ApJ, 678, 24
Meier, D. S., & Turner, J. L. 2005, ApJ, 618, 259
Mendoza, E., Lefloch, B., López-Sepulcre, A., et al. 2014, MNRAS, 445, 151
Mladenovic, M., Lewerenz, M., McCarthy, M. C., & Thaddeus, P. 2009, J. Chem.
  Phys., 131, 174308
Nguyen, T., Fourré, I., Favre, C., et al. 2019, A&A, 628, A15
Noble, J. A., Theule, P., Congiu, E., et al. 2015, A&A, 576, A91
Pirim, C., & Krim, L. 2011, PCCP, 13, 19454
Raghavachari, K., Trucks, G. W., Pople, J. A., & Head-Gordon, M. 1989, Chem.
  Phys. Lett., 157, 479
Redondo, P., Pauzat, F., Markovits, A., & Ellinger, Y. 2020, A&A, 638, A125
Redondo, P., Pauzat, F., Markovits, A., & Ellinger, Y. 2021, A&A, 646, A163
Rodríguez-Almeida, L. F., Rivilla, V. M., Jiménez-Serra, I., et al. 2021, A&A,
  654
Rubin, R. H., Swenson, Jr., G. W., Benson, R. C., Tigelaar, H. L., & Flygare,
   W. H. 1971, ApJ, 169, L39
Snyder, L. E., & Buhl, D. 1972, ApJ, 177, 619
Stoecklin, T., Halvick, P., Hua-Gen, Y., & Ellinger, Y. 2018, MNRAS, 475, 2545
Theule, P., Borget, F., Mispelaer, F., et al. 2011, A&A, 534, A64
Tielens, A. G. G. M., & Hagen, W. 1982, A&A, 114, 245
Tielens, A. G. G. M., & Whittet, D. C. B. 1997, in Molecular Astrophysics:
  Probes and Processes, ed. E. F. van Dishoeck, (Kluwer, Dordrecht, Proc. IAU
  Symp., 178), 45
Tieppo, N., Pauzat, F., Parisel, O., & Ellinger, Y. 2023, MNRAS, 518, 3820
```

Turner, B. E., Terzieva, R., & Herbst, E. 1999, ApJ, 518, 699

Zhao, Y., & Truhlar, D. G. 2008, Theor. Chem. Acc., 120, 215

Watanabe, N., & Kouchi, A. 2002, ApJ, 571, L173

Appendix A: Synthesis of the first amide NH₂CHO by hydrogenation of isocyanic acid HNCO on ice

Table A.1. Critical points on the hydrogenation path from HNCO into the final product NH₂CHO.

method *	n	CCSD(T)*/B1	CCSD(T)*/B2	M062X/B3	MPWB1K/B3
$H-nH_2O(^2A) + HNCO(^1A') + H(^2S)$	1	0.0	0.0	0.0	0.0
	2	0.0	0.0	0.0	0.0
	3	0.0	0.0	0.0	0.0
$H-Layer(^1A) + HNCO(^1A') + H(^2S)$	48			0.0	0.0
$\overline{\text{IR1 H} - \text{nH}_2\text{O} - \text{HNCO}(^2\text{A}) + \text{H}(^2\text{S})}$	1	-3.2		-3.0	-5.0
	2	-6.5		-6.2	-3.9
	3	-6.5		-6.0	-3.9
IR1 H $-$ Layer $-$ HNCO(2 A) $+$ H(2 S)	48			-13.3	-11.2
$NH_2CO - nH_2O(^2A) + H(^2S)$	1	-53.4	-53.6	-48.7	-52.3
	2	-57.1		-53.6	-54.6
	3	-55.9		-51.3	-53.5
$NH_2CO-Layer (^2A) + H (^2S)$	48			-56.7	-54.4
$HNCHO - nH_2O(^2A) + H(^2S)$	1	-32.6	-32.1	-27.0	-30.7
	2	-36.9		-32.5	-33.2
	3	-38.6		-31.2	-32.9
$HNCHO$ -Layer(^{2}A) + H (^{2}S)	48			-35.5	-34.0
$NH_2CHO-nH_2O(^1A)$	1	-146.6	-147.3	-142.0	-144.6
/	2	-150.8		-147.3	-147.4
	3	-149.4		-144.8	-146.0
NH ₂ CHO-Layer (¹ A)	48			-149.8	-146.7

^{*} The process implies that an hydrogen atom is first attached on the ice with an environment of n=1, 2, 3, and a double bi-layer of 48 water molecules. Geometries are optimized at the MP2/aug-cc-pVTZ level. Basis sets: B1=aug-cc-pVTZ; B2=aug-cc-pVQZ; n=number of supporting H_2O . Relative energies including zero-point vibrational energies in kcal/mol.